THE JOURNAL OF BIOLOGICAL CHEMISTRY
Vol. 279, No. 35, Issue of August 27, pp. 36354–36362, 2004
Printed in U.S.A.

Mapping Subunit Location on the *Saccharomyces cerevisiae* Origin Recognition Complex Free and Bound to DNA Using a Novel Nanoscale Biopointer*

Received for publication, March 30, 2004, and in revised form, June 15, 2004
Published, JBC Papers in Press, June 16, 2004, DOI 10.1074/jbc.M403501200

Paul D. Chastain II‡, Jayson L. Bowers§, Daniel G. Lee§¶, Stephen P. Bell§‖, and Jack D. Griffith‡**

From the ‡Lineberger Comprehensive Cancer Center, University of North Carolina, Chapel Hill, North Carolina 27599-7295 and the §Department of Biology, Howard Hughes Medical Institute, Massachusetts Institute of Technology, Cambridge, Massachusetts 02139

The *Saccharomyces cerevisiae* origin recognition complex (ORC) is composed of six subunits and is an essential component in the assembly of the replication apparatus. To probe the organization of this multiprotein complex by electron microscopy, each subunit was tagged on either its C or N terminus with biotin and assembled into a complex with the five other unmodified subunits. A nanoscale biopointer consisting of a short DNA duplex with streptavidin at one end was used to map the location of the N and C termini of each subunit. These observations were made using ORC free in solution and bound to the *ARS1* origin of replication. This mapping confirms and extends previous studies mapping the sites of subunit interaction with origin DNA. In particular, we provide new information concerning the stoichiometry of the ORC-*ARS1* complex and the changes in conformation that are associated with DNA binding by ORC. This versatile, new approach to mapping protein structure has potential for many applications.

The replication of eukaryotic DNA is dependent upon the timely and accurate formation of a series of multiprotein assemblies. The earliest of these events is the selection of potential sites for replication initiation within the genomic DNA. In bacteria, bacteriophages, and eukaryotic viruses this task is mediated by initiator proteins (1). In addition to identifying where to start replication, many initiator proteins facilitate the unwinding of the DNA helix at the replication origin and the recruitment of proteins that are needed to make a functional replisome (2).

It is widely accepted that the initiator for eukaryotic replication is the origin recognition complex (ORC)[1] (3). ORC was originally identified through its ability to bind to a conserved 11-bp sequence found at all *Saccharomyces cerevisiae* origins of replication called the autonomously replicating sequence (ARS) and autonomous consensus sequence (ACS) (reviewed in Ref. 4). These sequences are part of larger (100–150 bp) replication origins that include at least two other AT-rich elements (B1 and B2, see Refs. 5–7). ORC is composed of six subunits that are named in order of their relative size (Orc1–Orc6, largest to smallest). Although the replication origin structure in *S. cerevisiae* is more defined than that of many other eukaryotic organisms, ORC-related complexes have been identified and shown to be essential for DNA replication in many eukaryotic organisms including *S. cerevisiae*, *Schizosaccharomyces pombe*, *Drosophila melanogaster*, *Xenopus laevis*, and humans (reviewed in Ref. 8). Thus, ORC is likely to be a universal feature of eukaryotic DNA replication.

The interaction between ORC and DNA is a complex ATP-regulated event. Of the six ORC subunits, only Orc6 is dispensable for DNA binding (9). DNA cross-linking studies indicate that of the remaining five subunits four are in direct contact with origin DNA (Orc1, Orc2, Orc4, and Orc5). ORC binding to origin DNA requires ATP binding by its largest subunit, Orc1 (10). Orc1 is a slow ATPase that is inhibited when ORC binds to the ACS element of origin DNA. ORC also binds to ssDNA in a length-dependent but sequence- and ATP-independent manner (11). The minimum length of ssDNA ORC can bind is 30 bases, and the affinity increases until it reaches a maximum for sequences over 80 bases. Most interestingly, ssDNA stimulates ORC ATP hydrolysis with the same length dependence.

Electron microscopic studies of ORC suggest that its conformation changes depending on the DNA to which it is bound. When ORC is visualized by itself or bound to origin DNA, it appears to have two major globular domains (similar to a peanut shell) (11) (Fig. 1*A*). In contrast, ORC bound to ssDNA assumes a bent conformation (similar to a cashew) (11). Although the consequences of these changes in conformation are unknown, they could represent an altered ability of ORC to interact with other DNA replication factors or other intermediates in the replication initiation process.

To investigate further the architecture of ORC, it would be desirable to map the location of the six ORC subunits in the peanut-shaped particle and relate this information to previous DNA binding data. We initiated such a study by using antibodies tagged with gold particles, but we found that these gold antibody particles were too large to provide the needed resolution. Furthermore, this approach relied on the availability of high specificity antibodies with a low background of nonspecific binding. Thus, in a complex such as ORC, it would be difficult to obtain six different antibodies each with the same specificity and affinity. The requirement for different antibodies for each

* This work was supported in part by National Institutes of Health Grants GM31819, GM19014 (to J. G.), and GM52339 (to S. B). The costs of publication of this article were defrayed in part by the payment of page charges. This article must therefore be hereby marked "*advertisement*" in accordance with 18 U.S.C. Section 1734 solely to indicate this fact.

¶ Present address: Dept. of Molecular Biology, Massachusetts General Hospital, Boston, MA 02114.

‖ Supported by the Howard Hughes Medical Institute.

** To whom correspondence should be addressed. Tel.: 919-966-2151; Fax: 919-966-3015; E-mail: jdg@med.unc.edu.

[1] The abbreviations used are: ORC, origin recognition complex; BCCP, biotin carboxyl carrier protein; nt, nucleotide(s); ssDNA, single-stranded DNA; ARS, autonomously replicating sequence; ACS, autonomous consensus sequences.

subunit also makes gold antibody probes ill-suited to compare the relative accessibility of one subunit over another on the surface of the particle. These limitations led us to consider a more ideal nanoscale probe (which we will refer to as a biopointer) as follows: 1) would be simple to generate in ample amounts; 2) would have dimensions allowing visualization by routine EM preparative methods, although not being so large as to obscure its target; 3) would have a distinct appearance; 4) would have a high affinity for the target and a low background of nonspecific binding to DNA or proteins; and 5) could be used for different samples.

In this study we describe the design and synthesis of a novel DNA biopointer that satisfies these requirements and its use in mapping the location of the *S. cerevisiae* ORC subunits. The approach relies on the high affinity biotin-streptavidin association and methods to engineer proteins with peptide tags at their N or C termini which become biotinylated *in vivo* by biotin ligases when the proteins are expressed in bacteria (12–14), yeast (15), or insect cells (16). The biopointer itself is constructed from a 179-bp DNA to which a single streptavidin tetramer is bound at one end. The short DNA-streptavidin biopointer is easily distinguished by EM and has a relatively small cross-section and hence does not obscure its target. In this study we describe the use of this biopointer to map the relative location of ORC subunits within the complex in the presence and absence of origin DNA. Our findings have important implications for the stoichiometry of ORC bound to DNA and the conformational changes that occur during DNA binding.

EXPERIMENTAL PROCEDURES

Biotinylated ORC Complexes—To generate ORC complexes with a single subunit biotinylated at its C or N terminus, the last 88 residues of the acetyl-CoA carboxylase, BCCP subunit (SMEAPAAAEISGHIVRSPMVGTFYRTPSPDAKAFIEVGQKVNVGDTLCIVEAMKMMNQIEADKSGTVKAILVESGQPVEFDEPLVVIE) (17), plus a two-amino acid linker (GG) were placed on either the C or N terminus of each ORC subunit, and that ORC subunit along with the remaining five nontagged subunits were expressed in insect cells (18) and purified as described (9).

Biopointers—A 179-bp region of pBluescript® II S/K (+) phagemid vector (Stratagene, Inc.) between the T7 and T3 promoters was amplified by PCR using a 20-nucleotide biotinylated oligonucleotide (5′-bio-AAT TAA CCC TCA CTA AAG GG-3′), which overlies the T3 promoter, and a 22-oligonucleotide (5′-GTA ATA CGA CTC ACT ATA GGG C-3′), which overlies the T7 promoter. The resulting DNA fragments were extracted twice with phenol/chloroform, precipitated with ethanol, and resuspended in 10 mM Tris-HCl, pH 7.5, 1 mM EDTA (TE). The DNA fragment was further purified by electrophoresis on a 1% agarose gel run in 90 mM Tris base, 90 mM boric acid and eluted from the gel using a Qiacut kit (Qiagen). To form the biopointers, 1 μg of the DNA in TE was incubated with a 4-fold molar excess of streptavidin tetramers (Invitrogen) for 20 min at room temperature. Excess streptavidin was removed by filtration through a Clontech (Palo Alto, CA) Chroma-Spin+TE-100 column using the procedure specified by the manufacturer. For some preparations, DNA lacking bound streptavidin and dimers consisting of two DNAs bound to a single streptavidin were removed by banding in a CsCl density gradient for 36 h at 58,000 rpm at an average density of 1.6 g/ml.

DNA Containing the ARS1 Sequence—pARS1WT plasmid DNA (11) was digested with SpeI and EcoRV to generate a 2.2-kb fragment that contained the *ARS1* sequence and was purified as described by Lee and Bell (9).

Formation of ORC-Biopointer and ORC-Biopointer-DNA Complexes—Biopointers were incubated with purified ORC particles in 50 μl of binding buffer (20 mM HEPES-KOH, pH 7.6, 2 mM EDTA, 5 mM magnesium acetate, 0.15 M KCl) containing 100 μM ATP, 530 fmol of ORC (based on a molecular weight of 414,600 Da), and 1360 fmol of biopointers (based on a molecular mass of 184,100 Da). Following an overnight incubation at 4 °C, the samples were fixed with glutaraldehyde (0.6% final concentration) for 5 min at room temperature and then filtered through a Chroma-Spin+TE-100 column. Mixtures of ORC and the DNA fragment containing the *ARS1* were incubated in 50 μl of binding buffer, containing 138 fmol of ORC, 138 fmol of the dsDNA, and 100 μM ATP at room temperature for 10 min. Glutaraldehyde was then added to a final concentration of 0.3% for 3 min at room temperature, followed by filtration through a Chroma-Spin+TE-100 column. To 50 μl of elution buffer, 1360 fmol of biopointers was added and the mixture gently rocked overnight at 4 °C.

Electron Microscopy—The complexes above were adsorbed to thin carbon foils, washed, air-dried, and rotary shadowcast with tungsten at high vacuum (19). Samples were examined in a Phillips CM12 at 40 kV. Images of a large number of tagged ORC complexes for analysis were captured digitally using a Gatan 794 CCD camera attached to the CM12 and Digital Micrograph 3.3 (Gatan Inc., Pleasanton, CA). Images for publication were captured on sheet film, scanned with a Nikon LS4500 film scanner, the contrast optimized, and panels arranged using Adobe Photoshop software.

RESULTS

Generating a Nanoscale Biopointer—The biopointer generated here consisted of a 179-bp DNA containing biotin at one end to which a single streptavidin tetramer is bound. DNA of this length is relatively straight and is easily visualized by tungsten shadowcasting methods utilized to visualize DNA-protein complexes. The DNA is produced by PCR amplification with one DNA primer being modified with an attached biotin. To place streptavidin at the end of the DNA, the DNA was incubated with a 4–10-fold molar excess of streptavidin tetramers for 1 h at room temperature, and the unbound streptavidin was removed by gel filtration and/or CsCl density banding (see "Experimental Procedures").

Electron microscopy confirmed the largely monomeric nature of the streptavidin coupling protocol. As shown in Fig. 1*B*, one end of the DNA, but never both, was bound by a protein particle whose size was consistent with that of a single streptavidin tetramer (based on mass estimates from previous studies). Following CsCl density banding fractions could be obtained approaching 99% monomeric biopointers with a low contamination of dimers (two DNAs bound to a single streptavidin) or DNA rods without streptavidin (as scored by EM, $n = 500$).

Visualization of S. cerevisiae ORC Associated with a Biopointer—To map the relative location of the ORC subunits, two variants of each of the *S. cerevisiae* ORC subunits were produced, one containing an 87-amino acid sequence at the C terminus and one with this tag at the N terminus. This sequence, a fragment of the *Escherichia coli* biotin carboxyl carrier protein (BCCP), was identified as a target for *in vivo* biotinylation (17). When expressed in insect cells, this tag is efficiently biotinylated (18). Twelve different ORC variants were generated (termed ORC1C, ORC1N, ORC2C, etc. to indicate a single biotin incorporated into the C or N terminus of just one of the six subunits) by co-infecting insect cells with five viruses, each expressing a nontagged subunit, and a sixth virus expressing an ORC subunit with the 87-amino acid tag at one end. These modified complexes were purified to homogeneity, and following incubation with streptavidin, the gel mobility shift assays indicated that greater than 90% of the particles contained biotin (data not shown).

To measure the level of nonspecific binding of the biopointers, untagged ORC was incubated with a 2-fold molar excess of biopointers for 24 h at 4 °C. The samples were fixed and unbound biopointers removed by gel filtration chromatography. Following preparation for EM (see "Experimental Procedures") only 1.8% ($n = 106$) of the ORC molecules had a biopointer attached. In contrast, 31% ($n = 134$) of complexes that included a C-terminal Orc4 tag had an associated biopointer. The biopointer detected approximately the same percentage of complexes for the remaining 11 biotin-modified ORCs. Because long incubations were required for optimal binding of the biopointers to DNA-bound ORC, similar 24-h incubations were used for biopointer binding to DNA-free ORC. However, efficient binding of the biopointers to free ORC particles was

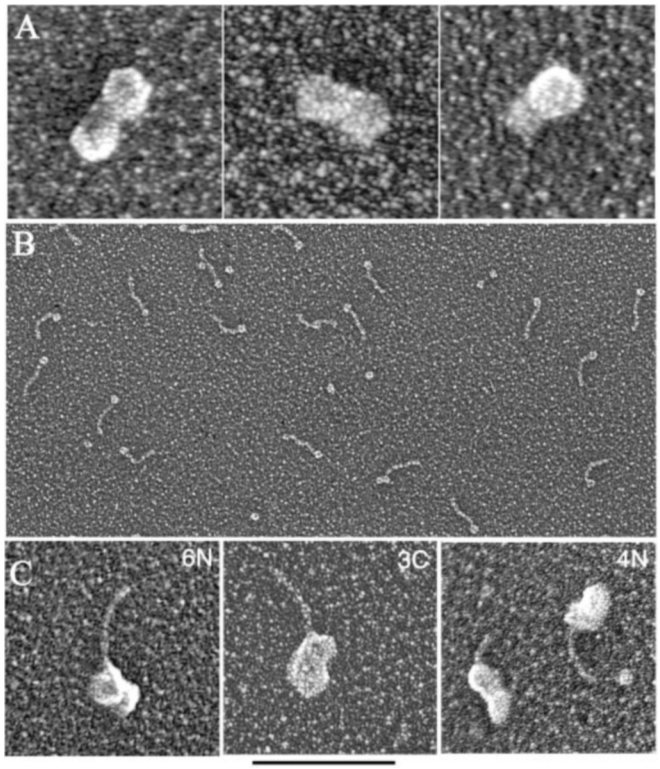

FIG. 1. **Visualization of ORC bound to a nano-scale biopointers.** *A*, following fixation, purified ORC particles were prepared for EM by mounting onto thin carbon foils, washing, and rotary shadowcasting with tungsten ("Experimental Procedures"). *B*, nano-scale biopointers consisting of a 179-bp DNA with a single streptavidin tetramer bound at one end were generated ("Experimental Procedures") and prepared for EM without fixation as above. Free balls are individual streptavidin tetramers present prior to removal by gel filtration. *C*, biotin can be placed at either the C or N terminus of one of the six ORC subunits with the other five subunits nonbiotinylated (see "Experimental Procedures"). Incubation of biotinylated ORC with the biopointers resulted in an association at a specific site. The biotinylated subunit is indicated the *upper right corner* of each panel and shown in reverse contrast. *Bar* is equivalent to 250 (*A*), 675 (*B*), and 200 bp (*C*).

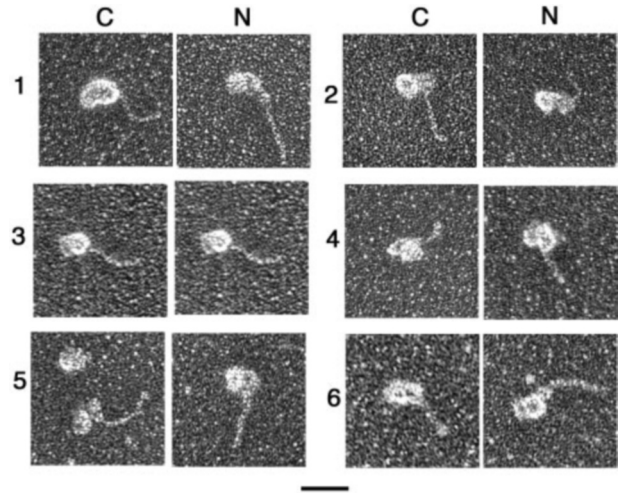

FIG. 2. **Gallery of biotinylated ORC variants associated with biopointers.** Each of the 12 biotinylated ORC variants was incubated with the biopointers and prepared for EM as in Fig. 1. The subunit number is shown to the *left* of each pair, and the C or N terminus designation is at the top. *Bar* equals a length of DNA equivalent to 200 bp.

observed after a 15-min incubation at room temperature (data not shown).

Examples of three different ORC variants with biopointers attached are shown in Fig. 1*C* at higher magnification, and a gallery of all 12 variants is shown in Fig. 2. ORC particles appeared bilobed as reported previously (11) (Fig. 1, *A* and *C*, and Fig. 2). Inspection of many images suggested that there is significant flexibility between the two lobes at the site of attachment. The two lobes appear joined asymmetrically so that as they lie on the EM support one long surface (denoted as the top) is "smooth" and the other surface (termed the bottom) has the shape of a rounded "w" (Fig. 1*A, left*). Following incubation with biopointers and preparation for EM, DNA tails were observed originating from the ORC particles at a single site (Fig. 1*C* and Fig. 2). The DNA tails exited ORC at different angles but never looped back. Examples could be seen in which the DNA rod was short, suggesting that ORC was lying over the biopointer. There was no indication that the biopointers oriented ORC in any one position on the EM grids.

Mapping the Location of ORC Subunits Using Biopointers—Because ORC has a distinct peanut-like shape with a top and bottom, mapping the point where the biopointers attach provides the potential for determining the location of each subunit within the particle. At least 50 examples of each of the 12 biotin-modified ORCs with biopointers attached were collected. To be included in the analysis the biopointers had to be nearly full length (to eliminate images in which ORC was lying on top of the biopointer), and the ORC particle had to have a bilobed morphology with a top and bottom. Because ORC was not bound to DNA in these experiments (see below), there was no means of determining left from right, but the smooth "top" and the w-shaped bottom surfaces provide a means of distinguishing one long surface from the other. As illustrated in Fig. 3*A*, the ORC particle was divided into four segments around the first half of a compass circle, (0–45, 46–90, 91–135, and 136–180°). Each ORC with a biopointer was placed in one of these four segments, and radial histograms were generated to provide a "radar view" (Fig. 3*B*). It is noteworthy that in only one case (ORC6C) was the percentage of complexes with two biopointers attached significantly above (2-fold) the background level (3–6%) of dimer biopointers in the background, and ORC6N was within this background level. This suggests that other than the possibility of ORC6, these subunits are present in only a single copy per complex. Furthermore, the results with DNA-bound ORC (see below) suggest that complexes with two ORC6 subunits may be nonfunctional.

As shown in the radar views, in several cases such as 1C, 4N, and 5C the distributions are narrow. In contrast, the locations determined for 2N, 3N, and 5N were broader, suggesting that these ends of these subunits were less tightly constrained. In general, the C-terminal distributions mapped close to the same quadrant as the N-terminal distributions.

Visualization and Mapping of ORC Subunit Location When Bound to Origin DNA—Observation of ORC bound to origin DNA offered an opportunity to gain additional information concerning the relative location of subunits within the complex and relative to the bound origin DNA. To this end, we repeated the experiments described above with ORC bound to a single copy of the *ARS1* origin of replication located asymmetrically within a DNA fragment. *ARS1* is located 33% from the nearest end of the fragment tested with the B elements located adjacent to the short end and the ACS adjacent to the long end (Fig. 4). Use of the biopointer in this context can address two important issues. First, although previous EM studies suggest that only one ORC binds to *ARS1*, the number of biopointers attached to each ORC·*ARS1* complex will definitively determine how many ORC molecules are bound at *ARS1* (and by extension other origins). Second, the presence of the asymmetric

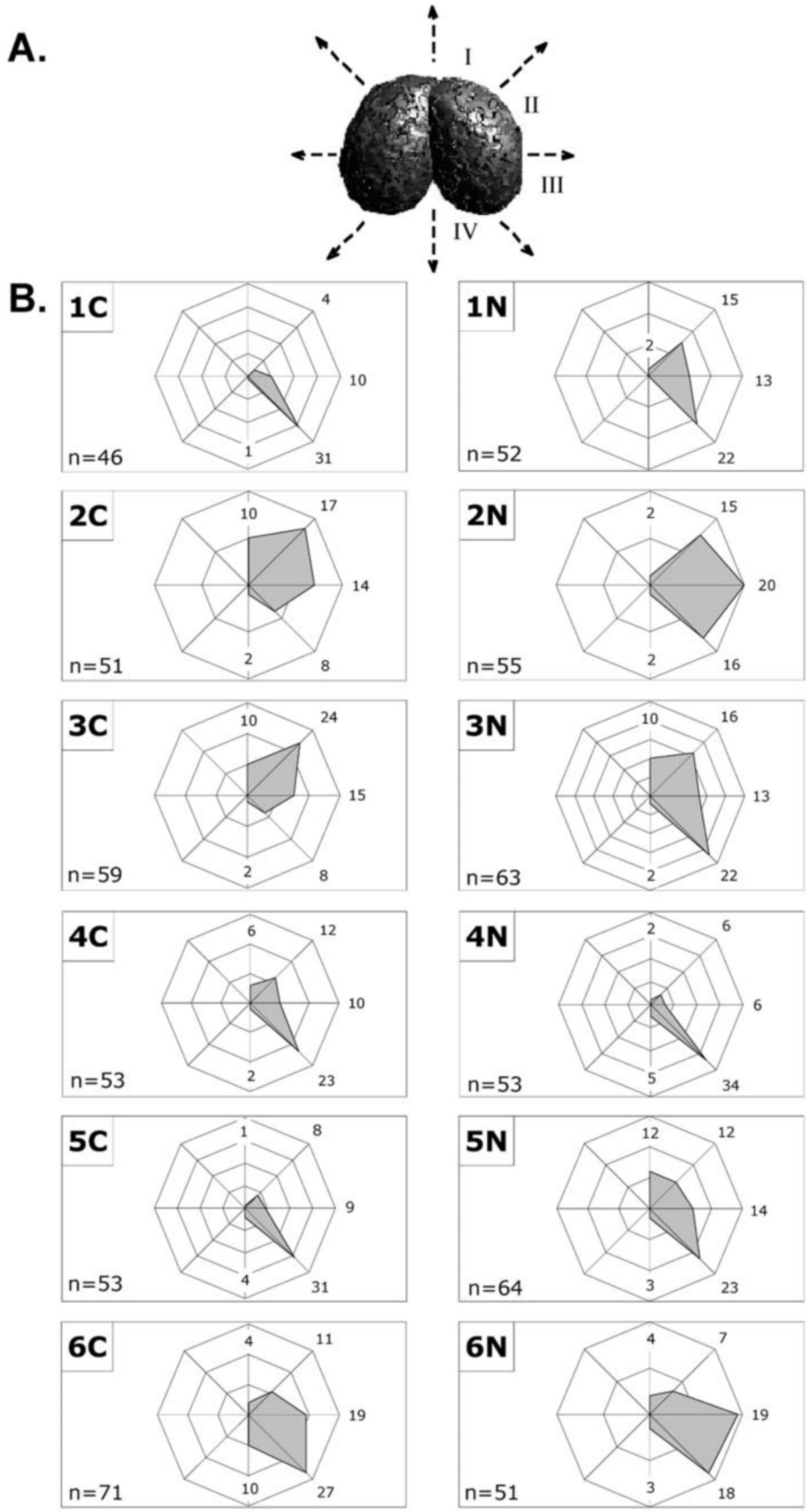

FIG. 3. **Radar view map of biopointer location on the ORC.** From the micrographs of free ORC we cannot distinguish left from right, but we can distinguish a smooth *top* surface from a lowercase w-shaped *bottom* surface. ORC was divided into four domains starting from the top of the molecule (domain I),and ending at the bottom (domain IV). *A*, to generate a radar view for each biotinylation site, the location at which a biopointer was attached was determined from electron micrographs as in Fig. 2 and placed in one of the four domains. *B*, to determine the percentage of biopointers associated within a particular domain, the number counted for each domain was divided by the total number of biopointers scored. The *gray* area of each radar view indicates the overall location to which all of the biopointers were mapped. The axial spokes define each domain area.

ARS1 DNA in these images allows the subunit location to be mapped relative to the elements of the origin.

To map the location of individual ORC subunits when bound to *ARS1* DNA, equimolar amounts of ORC and DNA were mixed at room temperature for 10 min and lightly fixed. At the ratio of ORCs to DNA used, only 33% of the DNA molecules were bound to ORC. Of the DNA molecules with ORC bound, roughly one-third appeared to be bound to the *ARS1* sequence

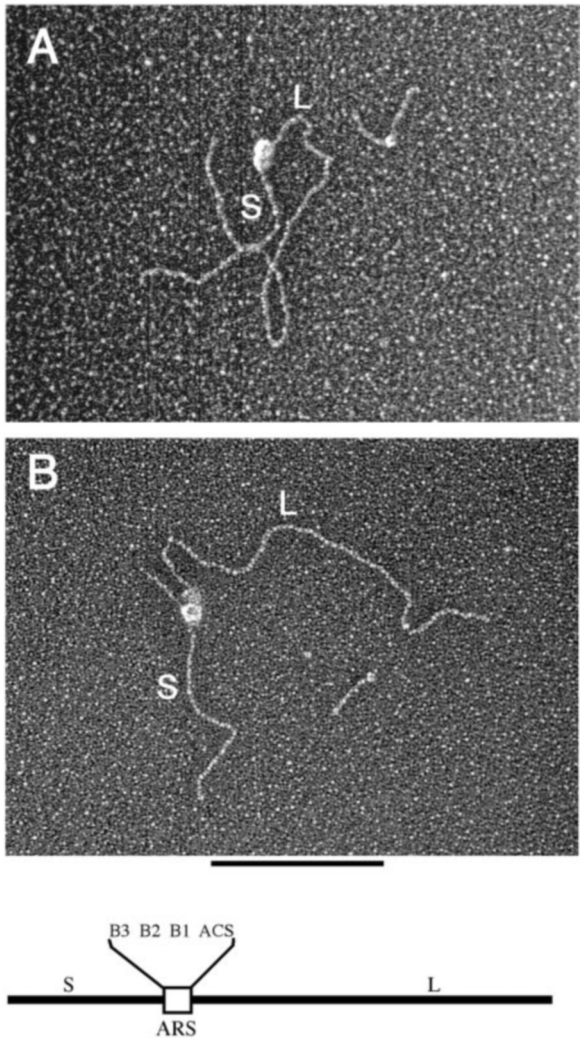

FIG. 4. **ORC bound to *ARS1* DNA.** Biopointers were incubated with complexes of ORC bound to a 2.2-kb fragment containing the *ARS1* element located 33% from one end. *A*, ORC was not biotinylated. *B*, the C terminus of Orc4p was biotinylated. The placement of the B3, B2, B1, and ACS regions within the *ARS1* element (*white box*) are denoted *above* the *ARS1* element. *ARS1* divides the DNA fragment into a short side (*S*) and a long side (*L*). *Bar* equals a length of DNA equivalent to 500 bp.

(~33% from one end). The remaining ORC-bound DNAs were split equally between those with ORC bound away from *ARS1* and those that were bound to more than one ORC molecule. Biopointers were never seen attached to the untagged ORC. When ORC was modified with biotin, however, we observed frequent association with a single biopointer (Fig. 4*B* and Fig. 5; Table I). We never observed a situation in which two biopointers were associated with ORC bound at the origin. The absence of such molecules strongly supports the hypothesis that ORC binds as a monomer to *ARS1* and that there is only one copy of each subunit within the bound complexes.

A gallery of micrographs of *ARS1*-bound ORC for each of the 12 different variants is shown in Fig. 5. In some cases the DNA was highly bent around the ORC (Fig. 5, *3N*, *5N*, and *4C*), but in other examples the DNA path was relatively straight (Fig. 5, *1C, 4N,* and *6C*). With long DNA arms used here, if the ORC binds to the support prior to the DNA arms, fluid flow can result in the DNA arms folding around the protein complex. Inspection of many examples did not show any consistent tendency for the ORC-proximal DNA to be bent, but bending of 45° or less could have been overlooked.

The efficiency of the biopointers attaching to a DNA-bound ORC was different for the 12 different ORC variants (Table I). This is in contrast to the situation when ORC was not bound to DNA in which case the efficiency was roughly the same for all 12 variants with ~30–35% of each ORC variant associated with the biopointer. In general the larger subunits (Orc1p, Orc2p, and Orc3p) were recognized by the biopointers more efficiently than the smaller subunits. The exception was the smallest subunit Orc6p, which was recognized as well as the larger subunits. Generally the efficiency of binding to the C or N termini was similar; however, there were marked differences for Orc2p and Orc5p. These differences in efficiency of biopointer binding most likely reflect the extent to which each terminus is buried in the ORC complex. Because this difference is more pronounced when ORC is bound to DNA, it suggests that either bound DNA or conformation changes in ORC upon DNA binding result in reduced accessibility of several of the termini.

A comparison of the ability of the biopointers to bind to a specific terminus when ORC was free in solution *versus* DNA bound could provide information about which subunit termini are blocked by DNA binding. To make this comparison, the tagged ORC variants were incubated with the *ARS1*-containing DNA fragment, and the sample was then lightly fixed and biopointers added. We then compared the fraction of free ORC associated with biopointers to the fractions of *ARS1*-bound ORC that were similarly associated. The results (Table II) show that in all cases DNA-bound ORC associated with the biopointer less efficiently than free ORC. Furthermore, there was a large variation in biopointer association efficiency depending on which ORC variant was tested. These findings suggested that DNA binding does mask some termini more than others. When the same comparison was made, including all DNA-bound ORCs (not just those at the *ARS1*), similar values were obtained (data not shown). This argues that the ORC makes similar contacts with DNA when it is bound away from the origin.

Using the smooth top and the w-shaped bottom surface of the ORC particle along with the asymmetric location of ORC along the DNA as a means to distinguish left from right, the point at which each biopointer was attached to *ARS1*-bound ORC was determined for at least 20 examples per ORC variant. As illustrated in Fig. 6, ORC was divided into eight 45° segments around the compass circle. Each DNA-bound ORC with a biopointer attached was placed in one of these eight segments, and radial histograms were generated to provide a radar view (Fig. 6). In several cases (1N, 4N, and 5N) the distributions are narrow as contrasted to 2N, 4C, and 6C that are broader. In general the C-terminal distributions map to the same radial segments as the N-terminal distributions. For example, the patterns of 5C and 5N overlap and map to similar radial wedges, suggesting that this subunit is locked into a single site on ORC with both termini being in close proximity. On the other hand, the distribution for 4N is narrow, whereas the distribution for 4C is broad, suggesting that whereas the N terminus may be specifically localized, the C terminus may be flexible and able to assume different positions over the surface of ORC.

DISCUSSION

In this study a novel EM procedure has been developed to map the location of the six subunits of the *S. cerevisiae* ORC. Each subunit was modified *in vivo* on either its C or N terminus with biotin and assembled into a complex with the five other unmodified subunits. A nanoscale biopointer consisting of a short stiff DNA with streptavidin at one end that could be seen in the EM was used to map the location of the C and N termini of each subunit in ORC. This was done for ORC free in solution

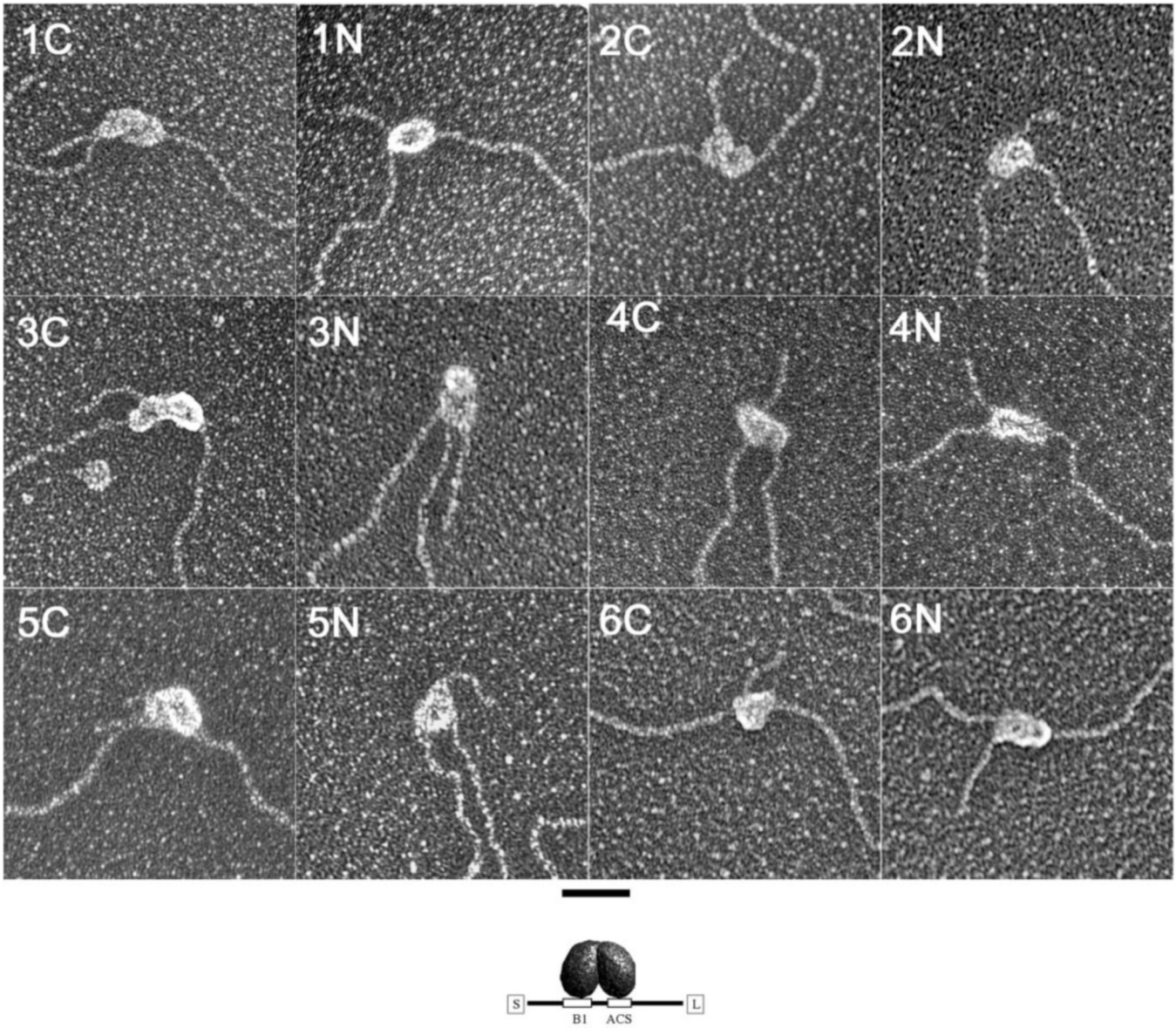

FIG. 5. **Gallery of ORC complexes at the *ARS1* associated with the biopointers.** Complexes of each of the 12 ORC variants were formed with the 2.2-kb fragment containing *ARS1* as in Fig. 4, incubated with the biopointers, and prepared for EM as in Fig. 1. The biotinylated subunit is indicated in each panel. The DNA-bound ORC is oriented such that the short side of the DNA fragment is on the *left side* of each micrograph. The bar equals a length of DNA equivalent to 500 bp.

TABLE I
Efficiency of biopointers labeling ARS1 bound ORCs

ORCs containing biotin on one terminus of a single subunit were incubated with the *ARS1* containing DNA fragment. For ORC bound to *ARS1* (33% from the nearest end), the presence or absence of a biopointer was scored to determine the efficiency of association.

		Location of Biotin	fraction of *ARS1* bound ORCs tagged	n =
ORC Subunit	1	C	26%	39
		N	30%	23
	2	C	47%	19
		N	14%	14
	3	C	41%	17
		N	30%	20
	4	C	6%	34
		N	11%	27
	5	C	12%	26
		N	25%	20
	6	C	25%	4
		N	23%	13

and bound to DNA at the *ARS1* origin of replication. The results of the mapping correspond well to previous chemical footprinting. More importantly, these findings provide new information concerning the stoichiometry of the ORC-*ARS1* DNA complex and support a model in which substantial conformational changes occur as ORC associates with origin DNA.

The biopointers are easily generated in ample amounts using PCR and a set of DNA primers, one of which is biotinylated. By using tungsten shadowcasting, the biopointers were easily distinguished from ORC and, in the case of DNA-bound ORC, from the bound *ARS1* DNA. The background of nonspecific binding of biopointers to nonbiotinylated ORCs was less than 2% at physiologic salt, and the biopointers should work well with other EM preparative methods. In studies by Nossal *et al.*,[2] biopointers were used to identify the presence and location of several bacteriophage T4 replication proteins within an active T4 replication complex and to estimate copy number. This

[2] N. Nossal, A. Makhov, P. D. Chastain II, and J. D. Griffith, unpublished data.

TABLE II
Ability of the biopointers to label a biotinylated ORC

To compare the relative availability of an ORC subunit terminus for the biopointers when ORC was free in solution or bound to *ARS1*, ORCs containing biotin on one terminus of a single subunit were incubated with DNA containing *ARS1*. Fields of molecules contained ORC particles that were both bound to *ARS1* and free in solution. In such fields the number of ORC particles that were labeled with a biopointer for these two classes was counted. ORC that was not bound to *ARS1* was not included in this scoring.

	Location of Biotin	ORC bound to *ARS1*	ORC free in solution	number scored	ratio: free verses DNA-bound
1	C	10	89	99	9
	N	7	121	128	17
2	C	9	50	59	6
	N	2	171	173	86
3	C	7	155	162	22
	N	6	246	252	41
4	C	2	179	181	90
	N	3	196	199	65
5	C	3	437	440	146
	N	5	230	235	46
6	C	1	623	624	623
	N	3	102	105	34

approach opens the door to both detection of a protein in a multiprotein complex and quantitative measurements of copy number and relative accessibility of each subunit to the surface. An additional advantage is that a single preparation of biopointers can be used for different biotinylated proteins as contrasted to gold antibody probes that must be generated anew for each target. Biopointers can also be used to map sites on RNA molecules to which biotinylated oligonucleotides are annealed, as revealed by Fouche *et al*.[3] in which the telomerase template region of yeast TLC1 RNA was localized by using a biopointer.

When ORC was bound to *ARS1* DNA, significant differences in the fraction of particles associated with a biopointer were observed depending on which subunit and which terminus contained the biotin. As shown in Table I, there was a greater than 8-fold difference depending on whether the biotin was on the C terminus of Orc2p (high binding) or the C terminus of Orc4p (low binding). There was also a 3-fold difference for Orc2p between the C terminus (high) and N terminus (low). Specifically, the ability of the biopointer to recognize its target was high (41–47% of the ORCs bound to DNA contained a biopointer) for ORC2C and ORC3C, lower (25–30%) for ORC1C, ORC1N, ORC3N, ORC5N, ORC6N, and ORC6C, (25–30%), and much lower (6–14%) for ORC2N, ORC4N, and ORC5C (Table I). These quantitative differences must reflect the relative accessibility of each biotinylated terminus to the biopointers, and thus provide a measure of the degree to which each terminus is either buried within ORC or lies at or near the surface of the particle. These data provide another level of structural information that can be derived by using biopointers that could not be obtained by using conventional gold antibody probes. Furthermore, it can be correlated with footprinting studies as described below.

In these experiments roughly 1/2 and 1/3 of the tagged ORC4N and ORC6C variants, respectively, had two biopointers attached (based on the observation above that roughly 30% of the 12 variants were tagged with a biopointer). Although this may suggest that a fraction of ORC reconstituted *in vivo* contains multiple copies of Orc4p and Orc6p, if so we would have expected to observe a higher frequency of double tagging for the opposite termini of the same two subunits. A second observation that calls into question the dimeric nature of these subunits is that none of the ORC variants showed significant double labeling when ORC was bound to *ARS1* DNA (see below), suggesting that particles with multiple copies of any subunit were excluded from DNA binding. Despite this, the interactions observed could represent potential interactions between subunits that could occur if more than one ORC were present at the origin at some point during the replication process.

The location of the subunit termini as determined by the biopointer approach correlates with and adds to previous ORC-DNA cross-linking studies (9). In these studies a cross-linker was placed at a variety of specific positions along *ARS1* DNA, and the ORC subunits that were within ~10 Å of the cross-linker were determined. This analysis provided a map of the subunits adjacent to each tested position. Consistent with these previous studies, we observed that both termini of Orc5 and the C terminus of Orc6 are located near the B-element side of *ARS1*. Similarly, biopointer localization indicates that the Orc1 and Orc2 N termini localize to the ACS end of *ARS1*, which is also consistent with the earlier cross-linking studies. These studies also add to these previous observations. Because the cross-linking studies can only monitor the parts of ORC adjacent to the DNA, they are unable to look more fully at the distribution of the proteins throughout the complex. For example, although the cross-linking studies indicated that the Orc6 subunit is restricted to the B-element side of ORC bound to *ARS1* DNA, the analysis with the biopointer suggests that Orc6 reaches between the two lobes of ORC. Similarly, Orc1 also appears to reach across the two lobes, despite being tightly restricted to the ACS side of *ARS1*-bound ORC in the protein-DNA cross-linking studies.

A second strong point of the biopointer approach is the ability to provide information concerning the stoichiometry of the protein-DNA complex. Although previous studies of ORC interactions with origin DNA generally supported the idea that a single ORC complex is bound to each origin (9, 11), in no case has this been shown definitively. The presence of only a single biopointer per ORC complex associated with origin DNA provides strong evidence that a single ORC is associated with each

[3] N. Fouche, D. Zappulla, T. Cech, and J. Griffith, unpublished data.

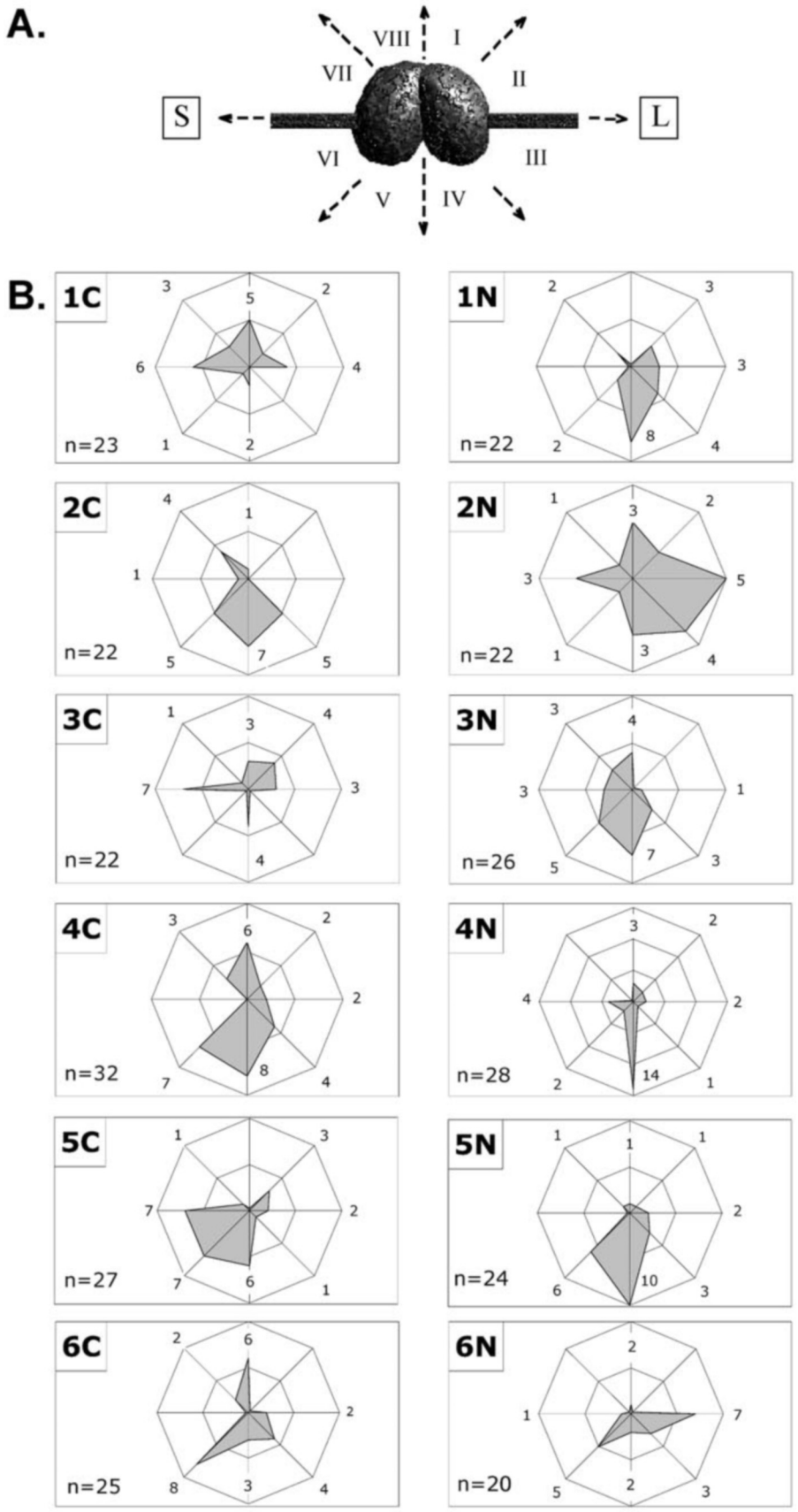

FIG. 6. **Radar view map of biopointer location on biotinylated ORC bound to *ARS1*.** *A*, ORC bound to *ARS1* was divided into eight equal 45° segments around the compass circle. The *top* and *bottom* designations are as in Fig. 5, and the side of ORC adjacent to the short segment of the DNA was placed on the *left*. Each of the 12 ORC variants was incubated with DNA followed by addition of biopointers and preparation for EM as in Fig. 5. *B*, to generate a radar view map for each tagged variant, the location where a biopointer was attached was determined from electron micrographs as in Fig. 5 and placed in one of the eight domains. At least 20 examples were scored for each map. The number of molecules scored for each domain was divided by the total number scored to determine the percent of molecules within that domain. The *gray* area of each radar view indicates the overall location to which all of the biopointers were mapped. The axial spokes define each domain.

origin. Similarly, these studies also support the hypothesis that there is only one copy of each subunit in each complex.

Comparison of the location of ORC subunits with and without *ARS1* DNA also suggests that some subunit termini change their locations significantly when bound to DNA. For example, the C terminus of Orc1 moves from a well defined "lower" position within the complex in the absence of *ARS1* to a more distributed position in the "upper" portion of ORC when it

binds DNA. In contrast, the C terminus of Orc2 moves from the upper to the lower portion of ORC upon DNA binding. Both of these findings support a model in which the conformation of ORC is altered significantly upon DNA binding. Such changes could facilitate binding of other replication proteins to ORC only when it is bound to origin DNA or it could regulate other activities of ORC that are altered when bound to origins (*i.e.* ATPase activity).

Together, these studies illustrate the power of using a well defined molecular pointer to characterize proteins and protein-DNA complexes by using electron microscopy. A significant limitation in this particular study arose from the apparent 2-fold symmetry of ORC, which made it impossible to distinguish between the left and right sides of ORC when free in solution. Furthermore, the distribution of pointer placement in some of the radar plots was broad thus making a precise determination of the subunit location difficult. Even with these limitations, our study has illustrated the potential of this approach to determine subunit stoichiometry and to provide insights into the general location of individual proteins in a larger complex. A major hurdle was the need to modify the target proteins or DNA with biotin. Although in this study the modification was performed *in vivo* after the addition of a 78-amino acid biotinylation tag to each subunit, in other instances chemical modification of specific residues (*e.g.* Cys) could be used to accomplish the same outcome. Smaller amino acid tags have now been identified (12) that could be used in place of the 88-amino acid sequence used here. Recently one of us (J. D. G.) generated C-terminal biotinylated TRF1 protein in insect cells using a 13-amino acid tag that was biotinylated when *E. coli* biotin ligase was co-expressed in the insect cells. In the future other temporal orders of coupling the pointer DNA to streptavidin may prove useful. In our work[2] on T4 replication complexes, we found that a higher level of tagging could be achieved if free streptavidin was first incubated with the replication complexes containing a biotinylated T4 DNA polymerase, followed by removal of the free streptavidin and then adding the pointer DNA. Finally, this general approach could be extended to generate biopointers specific for other protein epitopes (*e.g.* hexahistidine) We are constructing such a pointer at this time. The ability to double label complexes, for example by using a hexahistidine-specific pointer with a 300-bp-long DNA tail and a biotin-specific pointer with a 179-bp tail, would add greatly to the general power of this approach. We anticipate that the use of these nanoscale pointers will be applicable to many other situations, including the analysis of more complex assemblies of multiple proteins and DNA/RNA and higher resolution EM.

Acknowledgment—We thank Jeff Gelles for providing a plasmid containing the C-terminal fragment of *E. coli* BCCP used in the biotin modification studies.

REFERENCES

1. Stenlund, A. (2003) *Nat. Rev. Mol. Cell Biol.* **4,** 777–785
2. Mendez, J., and Stillman, B. (2003) *BioEssays* **25,** 1158–1167
3. Bell, S. P. (2002) *Genes Dev.* **16,** 659–672
4. Bell, S. P. (1995) *Curr. Opin. Genet. Dev.* **5,** 162–167
5. Marahrens, Y., and Stillman, B. (1992) *Science* **255,** 817–823
6. Rao, H., and Stillman, B. (1995) *Proc. Natl. Acad. Sci. U. S. A.* **92,** 2224–2228
7. Theis, J. F., and Newlon, C. S. (1994) *Mol. Cell. Biol.* **14,** 7652–7659
8. Bell, S. P., and Dutta, A. (2002) *Annu. Rev. Cell Biol.* **71,** 333–374
9. Lee, D. G., and Bell, S. P. (1997) *Mol. Cell. Biol.* **17,** 7159–7168
10. Klemm, R. D., and Bell, S. P. (1997) *Cell* **88,** 493–502
11. Lee, D. G., Makhov, A. M., Klemm R. D., Griffith, J. D., and Bell, S. P. (2000) *EMBO J.* **19,** 4774–4782
12. Schatz, P. J. (1993) *Bio/Technology* **11,** 1138–1143
13. Kim, D. R., and McHenry, C. S. (1996) *J. Biol. Chem.* **271,** 20690–20698
14. Beckett, D., Kovaleva, E., and Schatz, P. J. (1999) *Protein Sci.* **8,** 921–929
15. Hirata, T., Iwamoto-Kihara, A., Sun-Wada, G. H., Okajima, T., Wada, Y., and Futai, M. (2003) *J. Biol. Chem.* **278,** 23714–23719
16. Duffy, S., Tsao, K.-L., and Waugh, D. S. (1998) *Anal. Biochem.* **262,** 122–128
17. Cronan, J. E. (1990) *J. Biol. Chem.* **265,** 10327–10333
18. Berliner, E., Mahtani, H. K., Karki, S., Chu, L. F., Cronan, J. E., and Gelles, J. (1994) *J. Biol. Chem.* **269,** 8610–8615
19. Griffith, J. D., and Christiansen, G. (1978) *Annu. Rev. Biophys. Bioeng.* **7,** 19–35